Inorganic Chemistry
Article

*Inorg. Chem.* **2011**, *50*, 437–443 **437**
DOI: 10.1021/ic100980x

# Crystal Structures and Magnetic Properties of Nickel Complexes with Hydrotris(pyrazolyl)borate Ligand and Double Bridged by Phosphate Esters

**Luisa López-Banet, M. Dolores Santana,* and Gabriel García**

*Departamento de Química Inorgánica, Universidad de Murcia, E-30071 Murcia, Spain*

**Luis García and José Pérez**

*Departamento de Ingeniería Minera, Geológica y Cartográfica, Área de Química Inorgánica, Universidad Politécnica de Cartagena, E-30203 Cartagena, Spain*

**Teófilo Rojo and Luis Lezama***

*Departamento de Química Inorgánica, Facultad de Ciencia y Tecnología, Universidad del País Vasco, E-48080 Bilbao, Spain*

**Jean-Pierre Costes**

*Laboratoire de Chimie de Coordination du CNRS, UPR 8241, liée par conventions à l'Université Paul Sabatier et à l'Institut National Polytechnique de Toulouse, 205 route de Narbonne, 31077 Toulouse Cedex, France*

Received May 17, 2010

The reaction between $[NiTp^*(\mu\text{-}OH)]_2$ (Tp* = hydrotris(3,5-dimethylpyrazolyl)borate) and $(RO)_2P(O)OH$ (R = Et, Bu, 4-$NO_2$-Ph) affords the dinuclear nickel phosphates $[NiTp^*(\mu\text{-}O_2P(OR)_2)]_2$ (R = Et (**1**), Bu (**2**), 4-$NO_2$-Ph (**3**)), which have been studied by spectroscopic methods (IR, UV−vis, and $^1$H NMR). In chloroform solution, those complexes exhibit isotropically shifted $^1$H NMR resonances. Their molecular structures reveal that they all have an eight-membered $Ni_2O_4P_2$ ring which possesses two nickel centers bridged to each other by two isobidentate phosphate ligands. Magnetic studies on **1**−**3** and other similar complexes (**4** and **5**) reveal antiferromagnetic behavior at low temperatures as well as an interesting correlation between calculated *D* values and the planarity of eight-membered $Ni_2O_4P_2$ rings.

## Introduction

Phosphate esters are plentiful in nature and play critical roles in key biological processes such as cell growth, proliferation and differentiation, metabolism, cell signaling or gene expression.[1] Synthesis of polynuclear complexes with organophosphate bridging ligands has become an active area of research, mainly because of their relevance in biological systems[2] and the increasing interest in the search of molecule-based and single molecule magnets.[3] Magnetostructural correlations depend on the superexchange coupling (*J*) between the spins of unpaired electrons located at metal atoms and connected through bridging ligands or interacting units.[4] Coupling in this kind of systems may be modulated in two ways: on the one hand, by change of co-ordination geometry of polyhedra and, therefore, the environment of the metal ions or, on the other hand, by means of variations in bonding parameters related to the bridging ligand.[3a] But these modifications affect not only the magnitude of the exchange coupling but also the magnetic anisotropy of the single metal ions that determines the magnetic behavior of these systems. In this sense, zero-field splitting of octahedral Ni(II) compounds and the consequences on the magnetic properties have been extensively

*To whom correspondence should be addressed. E-mail: dsl@um.es (M.D.S.), luis.lezama@ehu.es (L.L.).

(1) Stivers, J. T.; Nagarajan, R. *Chem. Rev.* **2006**, *106*, 3443–3467.
(2) Feng, G.; Tanifum, E. A.; Adams, H.; Hengge, A. C.; Williams, N. H. *J. Am. Chem. Soc.* **2009**, *131*, 12771–12779.
(3) (a) Mukherjee, P.; Drew, M. G. B.; Gómez-García, C. J.; Ghosh, A. *Inorg. Chem.* **2009**, *48*, 5848–5860. (b) Kahn, O. *Molecular Magnetism*; VCH: New York, 1993; (c) Gatteschi, D.; Sessoli, R.; Villain, J. *Molecular Nanomagnets*; Oxford University Press: Oxford, U.K., 2006.
(4) (a) Ruiz, E.; Álvarez, S. *Chem. Phys. Chem.* **2005**, *6*, 1094. (b) Rodriguez, J. H.; McCusker, J. K. *J. Chem. Phys.* **2002**, *116*, 6253.


Published on Web 12/13/2010

studied.[5] Magnetic anisotropy of these compounds is mainly originated by second-order spin−orbit coupling between the ground and the excited states. Therefore, the magnitude of zero-field splitting ($D$) depends on the energy difference between ground and excited states as well as the degree of splitting of these ones. As the first contribution has only small variations for different hexacoordinate Ni(II) complexes, the observed magnetic anisotropy is usually related to the distortion in the coordination sphere of the metal center. In the reported data,[6] zero-field splitting parameters are usually lower than 10 $cm^{-1}$. For tetracoordinate Ni(II) complexes, $D$-values are much larger and strongly depend on the energy gap between the two levels of the corresponding $^3T_1$ ground state, which have non-zero orbital angular moment. $D$-values up to 50 $cm^{-1}$ have been detected in pseudotetrahedral Ni(II) complexes which have been proposed as models for N−S coordinated nickel enzymes.[7] The magnetic anisotropy of pentacoordinated Ni(II) compounds is expected to lie between the one that correspond to octahedral and distorted tetrahedral symmetry, but only a few studies have been reported to date[8] because of the scarcity of this coordination number in nickel systems. The aim of starting the study of five-coordinate dinuclear Ni(II) complexes of phosphate esters and Tp* anions, which still remain unexplored, is due to increase the knowledge about the influence of the structural parameters on their magnetic behavior. Accordingly, herein we report the synthesis, structure, and magnetic properties of the dinuclear nickel(II) phosphates [NiTp*($\mu$-$O_2P(OR)_2$)]$_2$ (R = Et (**1**), Bu (**2**), 4-$NO_2$-Ph (**3**)) and the magnetic properties of [NiTp*($\mu$-$O_2P(OMe)_2$)]$_2$ (**4**) and [NiTp*($\mu$-$O_2P(OPh)_2$)]$_2$ (**5**) as well, which have been prepared previously.[9]

## Experimental Section

**General Methods.** Infrared spectra were recorded on a Perkin-Elmer PRECISELY Spectrum 100 FT-IR Spectrometer using Nujol mulls between polyethylene sheets. The UV/vis spectra (in $CH_3Cl$) were recorded on a UNICAM UV 500 spectrophotometer equipped with matched quartz cells in the 240−850 nm range. The $^1$H NMR spectra were recorded on a Bruker model AC 200E. Accurate mass measurements were performed on an Agilent 6220 time-of-flight MS coupled to a HPLC Agilent series 1200 and equipped with an ionization source electrospray-APCI. The instrument was operated in the positive ion mode using a mass range of 25−20000 $m/z$. C, H, N analyses were performed with a Carlo Erba model EA 1108 microanalyzer. Magnetic susceptibilities of powdered samples were measured between 1.8 and 300 K with a Quantum Design MPMS-5 SQUID magnetometer in an external field of 0.1 T. The experimental susceptibilities were corrected for the diamagnetism of the sample-holders and the constituent atoms (Pascal tables) and for the temperature-independent paramagnetism estimated to be $100 \times 10^{-6}$ $cm^3$ $mol^{-1}$.[10] Isothermal magnetization measurements were performed up to 5 T at several temperatures between 2 and 20 K. Magnetic susceptibilities were computed by exact calculations of the energy levels associated with the spin Hamiltonian through diagonalization of the full matrix with the MAGPACK program package.[11]

**Materials.** All of chemicals were purchased from Aldrich and were used without further purification. Solvents were dried and distilled by general methods before use. The complex [NiTp*($\mu$-OH)]$_2$ (Tp* = hydrotris(3,5-dimethylpyrazolyl)borate) were prepared by previously described procedures.[12]

**Synthesis of [NiTp*($\mu$-$O_2P(OR)_2$)]$_2$ (R = Et (1), Bu (2), 4-$NO_2$-Ph (3)).** Complexes **1**−**3** were prepared by reaction of [NiTp*($\mu$-OH)]$_2$ (100 mg, 0.134 mmol) with the corresponding dialkyl or diaril phosphoric acid $(RO)_2P(O)OH$ (R = Et, Bu, 4-$NO_2$-Ph) (41.1 mg, 56.6 mg, 91.4 mg, respectively; 0.268 mmol) in chloroform (30 mL). After stirring for 30 min, the solution was evaporated under reduced pressured and $n$-hexane was added to the solution. The resulting green solid was collected by filtration, washed with $n$-hexane and air-dried. Single crystals for X-ray diffraction measurements were obtained by slow evaporation of a chloroform solution of the corresponding complex. Yields: 70 [**1**], 75 [**2**], 88 [**3**] %.

**[NiTp*($\mu$-$O_2P(OEt)_2$)]$_2$ (1).** TOF-MS ($m/z$) 1014.3368, calc ($C_{38}H_{64}B_2N_{12}Ni_2O_8P_2$) 1014.3411; [NiTp*($\mu$-$O_2P(OEt)_2$)]$_2$−($\mu$-$O_2P(OEt)_2$, 861.3125, calc ($C_{34}H_{54}B_2N_{12}Ni_2O_4P$) 861.3094; IR (nujol): 2511 $\nu$(B−H), 1546 $\nu$(C=N), 1275 $\nu_a(PO_2)$, 1131 $\nu$[(P)-O-C], 1062 $\nu_s(PO_2)$, 960 $\nu$[P-O-(C)], 465 $cm^{-1}$ $\nu$(Ni−O); UV−vis in chloroform: $\lambda$ (nm), ($\varepsilon$, $M^{-1}$ $cm^{-1}$): 681 (31.1), 412 (102.6); $^1$H NMR ($CDCl_3$, TMS): 67.6 (4-H-pz, 3H), 3.7 (−$OCH_2$, 4H), 1.2 ($CH_3$, 6H), −0.3 (5-Me, 9H), −9.8 (3-Me, 9H) ppm. Anal. Calcd for $C_{38}H_{64}B_2N_{12}Ni_2O_8P_2$: C, 44.84; H, 6.34; N, 16.51. Found: C, 44.67; H, 6.40; N, 16.29.

**[NiTp*($\mu$-$O_2P(OBu)_2$)]$_2$ (2).** TOF-MS ($m/z$) 1126.4678, calc ($C_{46}H_{80}B_2N_{12}Ni_2O_8P_2$) 1126.4663, [NiTp*($\mu$-$O_2P(OBu)_2$)]$_2$−($\mu$-$O_2P(OBu)_2$) 917.3688, calc ($C_{38}H_{62}B_2N_{12}Ni_2O_4P$) 917.372; IR (nujol): 2507 $\nu$(B−H), 1546 $\nu$(C=N), 1270 $\nu_a(PO_2)$, 1126 $\nu$[(P)-O-C], 1000 $\nu_s(PO_2)$, 910 $\nu$[P-O-(C)], 467 $cm^{-1}$ $\nu$(Ni−O); UV−vis in chloroform: $\lambda$ (nm), ($\varepsilon$, $M^{-1}$ $cm^{-1}$): 684 (40.5), 414 (130.3); $^1$H NMR ($CDCl_3$, TMS): 68.7 (4-H-pz, 3H), 3.7 (−$OCH_2$, 4H), 1.6 (−$CH_2$−, 4H), 0.9 (−$CH_2$−, 4H), 0.5 (−$CH_3$, 6H), 0.0 (5-Me, 9H), −9.7 (3-Me, 9H) ppm. Anal. Calcd for $C_{46}H_{80}B_2N_{12}Ni_2O_8P_2$: C, 48.89; H, 7.13; N, 14.87. Found: C, 48.95; H, 7.24; N, 14.72.

**[NiTp*($\mu$-$O_2P(OPh\text{-}4\text{-}NO_2)_2$)]$_2$ (3).** TOF-MS ($m/z$) 1386.2803, calc ($C_{54}H_{60}B_2N_{16}Ni_2O_{16}P_2$) 1386.2814, [NiTp*($\mu$-$O_2P(OPh\text{-}4\text{-}NO_2)_2$)]$_2$ - ($\mu$-$O_2P(OPh\text{-}4\text{-}NO_2)_2$)] 1047.2787, calc ($C_{42}H_{52}B_2N_{14}Ni_2O_8P$) 1047.279; IR (nujol): 2527 $\nu$(B−H), 1611, 1590 $\nu$(C=C), 1545, 1520 $\nu$(C=N), 1251, 1225 $\nu_a(PO_2)$, 1188 $\nu$[(P)-O-C], 1067 $\nu_s(PO_2)$, 914 $\nu$[P-O-(C)], 467 $cm^{-1}$ $\nu$(Ni−O); UV−vis in chloroform: $\lambda$ (nm), ($\varepsilon$, $M^{-1}$ $cm^{-1}$): 669 (50.8); $^1$H NMR ($CDCl_3$, TMS): 69.3 (4-H-pz, 3H), 7.9 (-OPh-4-$NO_2$, 8H), 0.2 (5-Me, 9H), −10.2 (3-Me, 9H) ppm. Anal. Calcd for $C_{54}H_{60}B_2N_{16}Ni_2O_{16}P_2$: C, 46.66; H, 4.35; N, 16.12. Found: C, 45.88; H, 4.20; N, 15.62.

**X-ray Data Collection and Structure Determination.** Diffraction data were collected in Oxford Diffraction Xcalibur (**3**) and

(5) (a) Carlin, R. L. *Magnetochemistry*; Springer-Verlag: Berlin, 1986; (b) Kahn, O. *Molecular Magnetism*; VCH: New York, 1993.
(6) (a) Boca, R. *Coord. Chem. Rev.* **2004**, *248*, 757–815. (b) Titis, J.; Boca, R. *Inorg. Chem.* **2010**, *49*, 3971–3973.
(7) Fryendahl, H.; Toftlund, H.; Becker, J.; Dutton, J. C.; Murray, K. S.; Taylor, L. F.; Anderson, O. P.; Tieking, E. R. T. *Inorg. Chem.* **1995**, *34*, 4467–4476.
(8) (a) Rebilly, J.-N.; Charron, G.; Rivière, E.; Guillot, R.; Barra, A.-L.; Serrano, M. D.; van Slageren, J.; Mallah, T. *Chem.—Eur. J.* **2008**, *14*, 1169–1177. (b) Jiménez, H. R.; Salgado, J.; J. M. Moratal, J. A.; Morgenstern-Badarau, I. *Inorg. Chem.* **1996**, *35*, 2737–2741. (c) van Albada, G. A.; Kolnaar, J. J. A.; Smeets, W. J. J.; Spek, A. L.; Reedijk, J. *Eur. J. Inorg. Chem.* **1998**, 1337–1341. (d) Vicente, R.; Escuer, A.; Solans, X.; Font-Bardía, M. *Inorg. Chim. Acta* **1996**, *248*, 59–65. (e) Kou, H.-Z.; Hishiya, S.; Satu, O. *Inorg. Chim. Acta* **2008**, *361*, 2396–2406.
(9) Pérez, J.; García, L.; Carrascosa, R.; Pérez, E.; Serrano, J. L.; Sánchez, G.; García, G.; Santana, M. D.; López, L.; García, J. *Z. Anorg. Allg. Chem.* **2007**, *633*, 1869–1874.
(10) Mabbs, F. E.; Machin, D. J. *Magnetism and Transition Metal Complexes*; Chapman and Hall: London, 1973.
(11) Borrás-Almenar, J. J.; Clemente-Juan, J. M.; Coronado, E.; Tsukerblat, B. S. *Inorg. Chem.* **1999**, *38*, 6081–6088. Borrás-Almenar, J. J.; Clemente-Juan, J. M.; Coronado, E.; Tsukerblat, B. S. *J. Comput. Chem.* **2001**, *22*, 985–991.
(12) Hikichi, S.; Yoshizawa, M.; Sasakura, Y.; Komatsuzaki, H.; Moro-oka, Y.; Akita, M. *Chem.—Eur. J.* **2001**, *7*, 5011–5028.

**Table 1.** Crystal Data and Structure Refinement Parameters for Compounds **1**−**3**

| | **1** | **2** | **3** |
|---|---|---|---|
| formula | $C_{38}H_{64}B_2N_{12}Ni_2O_8P_2$ | $C_{46}H_{80}B_2N_{12}Ni_2O_8P_2$ | $C_{54}H_{60}B_2N_{16}Ni_2O_{16}P_2$ |
| formula weight | 1024.04 | 1130.20 | 1390.16 |
| temperature/K | 100(2) | 100(2) | 100(2) |
| wavelength/Å | 0.71073 | 0.71073 | 0.71073 |
| crystal system | triclinic | tetragonal | monoclinic |
| space group | $P\bar{1}$ | $P42/mbc$ | $P21/n$ |
| $a$ /Å | 8.1475(6) | 16.533 | 9.6445(8) |
| $b$/Å | 11.5772(9) | 16.533 | 14.7369(18) |
| $c$/Å | 13.3096(10) | 20.512 | 21.543(2) |
| α/deg | 90.6430(10) | 90 | 90 |
| $\beta$/deg | 100.9280(10) | 90 | 92.990(8) |
| $\gamma$/deg | 97.5660(10) | 90 | 90 |
| $V$/Å$^3$ | 1221.09(16) | 5606.6 | 3057.7(5) |
| $Z$ | 1 | 4 | 2 |
| $d_{calcd.}$/ Mg/m$^{-3}$ | 1.393 | 1.339 | 1.510 |
| absorption coefficient/mm$^{-1}$ | 0.897 | 0.788 | 0.750 |
| $F$(000) | 542 | 2400 | 1440 |
| $\theta$ range/deg | 1.78 to 28.30 | 1.74 to 28.24 | 2.53 to 29.15 |
| index ranges | $-10 \le h \le 10$ | $-21 \le h \le 21$ | $-13 \le h \le 11$ |
| | $-15 \le k \le 15$ | $-21 \le k \le 21$ | $-19 \le k \le 20$ |
| | $-16 \le l \le 16$ | $-25 \le l \le 26$ | $-24 \le l \le 28$ |
| reflections collected | 14217 | 61075 | 21851 |
| independent reflections [$R_{int}$] | 5478 [0.0449] | 3478 [0.0351] | 7078 [0.0902] |
| max. and min transmission | 0.9736 and 0.7503 | 0.8909 and 0.8095 | 0.9779 and 0.8464 |
| data/restraints/parameters | 5478/24/289 | 3478/0/177 | 7078/0/415 |
| GoF on $F^2$ | 1.055 | 1.077 | 0.656 |
| final $R$ indices [$I > 2\sigma(I)$] | $R_1 = 0.0744$ | $R_1 = 0.0559$ | $R_1 = 0.0476$ |
| | $wR_2 = 0.1702$ | $wR_2 = 0.1519$ | $wR_2 = 0.0993$ |
| $R$ indices (all data) | $R_1 = 0.0934$ | $R_1 = 0.0598$ | $R_1 = 0.1456$ |
| | $wR_2 = 0.1812$ | $wR_2 = 0.1550$ | $wR_2 = 0.1136$ |
| largest diff. peaks [e Å$^{-3}$] | 1.179, −1.149 | 2.303, −0.578 | 1.004, −0.454 |

in Bruker Smart Apex (**1** and **2**) diffractometers with graphite-monochromated Mo-$K\alpha$ radiation ($\lambda = 0.71073$ Å). The diffraction frames were integrated using the SAINT package[13] and corrected for absorption with SADABS[14] for complexes **1** and **2**. The crystallographic data are shown in Table 1. The structures were solved by direct methods[15] and refined anisotropically on $F^2$.[15] Hydrogen atoms were introduced in calculated positions.

## Results and Discussion

**Synthesis and Spectroscopic Characterization.** Nickel hydroxo complexes have been regarded as versatile starting compounds for a variety of inorganic compounds because they are readily susceptible to dehydrative condensation with protic substrates (Ni-OH + H-A → Ni-A + $H_2O$). We have explored this reactivity in the hydroxo-complex $[Ni(C_6F_5)_2(\mu\text{-OH})]_2^{2-}$ synthesizing a wide variety of square planar Ni(II) complexes.[16] On the basis of this synthetic method, we have been reported the preparation of pentacoordinate nickel(II) complexes containing bridging phosphate esters or phosphinate ligands using the hydroxo-complexes $[Ni(mcN_3)(\mu\text{-OH})]_2(PF_6)_2$ [$mcN_3$ = 2,4,4-trimethyl-1,5,9-triazacyclododec-1-ene or 2,4,4,9-tetramethyl-1,5,9-triazacyclododec-1-ene), which also lead to hydrolytic processes toward phosphate triesters.[17] To continue with our work related to hydroxo nickel complexes, the reaction of $[NiTp^*(\mu\text{-OH})]_2$ toward dialkyl or diaryl phosphoric acids leads to the formation of green bis-(phosphate)-bridged dinuclear complexes $[NiTp^*\{\mu\text{-}O_2P(OR)_2\}]_2$ (R = Et (**1**), Bu (**2**) and 4-$NO_2$-Ph (**3**)) *via* acid−base reaction. The new complexes have been characterized by TOF mass spectrometry and spectroscopic (IR, UV−vis, $^1$H NMR) techniques. The IR spectra of **1**−**3** support the presence of the phosphate ligands, which show bands at 1131, 1126, 1188 and 960, 910, 914 cm$^{-1}$ which could be assigned to the $\nu$[(P)-O-C] and $\nu$[P-O-(C)] vibrations, respectively.[17,18] The bands due to $\nu_a(PO_2)$ and $\nu_s(PO_2)$ vibrations fall in the 1275−1225 and 1067−1000 cm$^{-1}$ ranges, respectively. IR spectra of **1**−**3** also show characteristic absorption of the tris(pyrazolyl)borate ligand[19] $\nu$(BH) at 2511, 2507, and 2527 cm$^{-1}$, respectively. All of the complexes exhibit relatively sharp hyperfine-shifted $^1$H NMR signals in chloroform solution spanning from 70 to −10 ppm. $^1$H NMR spectra of complexes **1**−**3** have been assigned on the basis of our previous studies of paramagnetic nickel(II) complexes[20] which consider not only chemical shift but also relative integration.[12,21] In all cases, Tp* arms are magnetically equivalent in solution. In general, the nearest protons to the nickel ion suffer the largest chemical shift as well as the greatest line broadening. Thus, 4-H protons from the pyrazolyl rings were observed at the largest downfield shift, around 68 ppm.

(13) *SAINT*, Version 6.22; Bruker AXS Inc.: Madison, WI
(14) Sheldrick, G. M. *SADABS*; University of Göttingen: Göttingen, Germany, 1996.
(15) Sheldrick, G. M. *SHELX-97, Programs for Crystal Structure Analysis*, release 97.2; University of Göttingen: Göttingen, Germany, 1998.
(16) Sánchez, G.; Ruiz, F.; Santana, M. D.; García, G.; López, G.; Hermoso, J. A.; Martínez-Ripoll, M. *J. Chem. Soc., Dalton Trans.* **1994**, 19–23, and references therein.
(17) Santana, M. D.; García, G.; Lozano, A. A.; López, G.; Tudela, J.; Pérez, J.; García, L.; Lezama, L.; Rojo, T. *Chem.—Eur. J.* **2004**, *10*, 1738.
(18) (a) Turowski, P. N.; Armstrong, W. H.; Liu, S.; Brown, S. N.; Lippard, S. J. *Inorg. Chem.* **1994**, *33*, 636–645. (b) Adams, H.; Bailey, N. A.; Fenton, D. E.; He, Q.-Y. *J. Chem. Soc., Dalton Trans.* **1997**, 1533–1539.
(19) Kujime, M.; Hikichi, S.; Akita, M. *Inorg. Chim. Acta* **2003**, *350*, 163–174.
(20) Santana, M. D.; López-Banet, L.; García, G.; García, L.; Pérez, J.; Liu, M. *Eur. J. Inorg. Chem.* **2008**, 4012–4018.
(21) Kitajima, N.; Hikichi, S.; Tanaka, M.; Moro-oka, Y. *J. Am. Chem. Soc.* **1993**, *115*, 5496–5508.

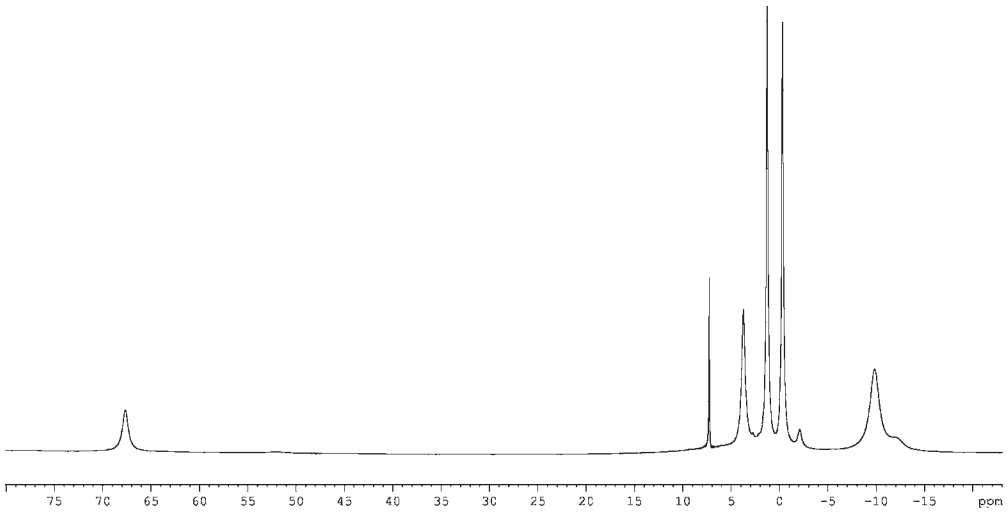


**Figure 1.** $^1$H NMR spectrum of **1** (in $CDCl_3$ solution at room temperature).

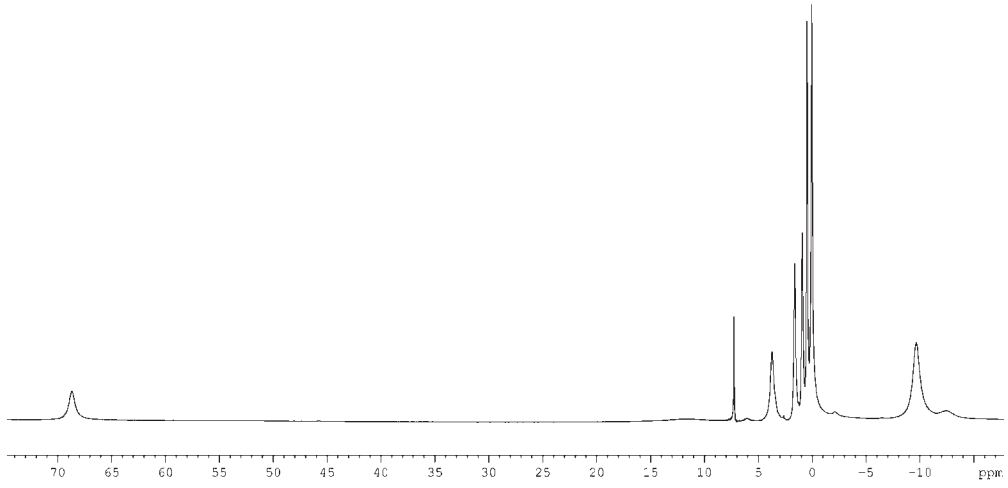


**Figure 2.** $^1$H NMR spectrum of **2** (in $CDCl_3$ solution at room temperature).

This tendency is general for complexes that contain hydrotris(pyrazolyl)borate ligand.[22] Methyl protons close to boron atom (5-Me) are observed between 0.2 and −0.3 ppm. However, signals of 3-Me protons that are near nickel ions are broadened and shift from diamagnetic position −9.7 to −10.2 ppm. Phosphate esters are far from nickel atoms, so that the resonances of their alkyl and aryl groups suffer smaller shift. These resonances are assigned to the remaining unassigned peaks and all of them are downfield to TMS (see Figures 1 and 2). This fact agree with a dominant $\sigma$-delocalization pattern of spin density and it is consistent with the presence of two unpaired electrons in $\sigma$-symmetry orbitals ($d_{x^2-y^2}$, $d_{z^2}$) of the ground state of nickel(II); however these unpaired electrons could polarize net spin density in $d_\pi$ orbitals,[23] behavior that has been also observed.[24]

**Solid State Structures of the Complexes.** Single-crystal X-ray diffraction study on [NiTp*($\mu$-$O_2P(OEt)_2$)] (**1**), [NiTp*($\mu$-$O_2P(OBu)_2$)] (**2**) and [NiTp*($\mu$-$O_2P(OPh\text{-}4\text{-}NO_2)_2$)] (**3**) confirms that phosphate anion, formed by deprotonation of the corresponding phosphoric acid, is bonded to nickel atoms as a bridging ligand. Selected bond lengths and angles for these complexes can be found in Table 2, whereas Figures 3−5 show the thermal ellipsoid diagrams. Dinuclear structures of **1**, **2**, and **3** are similar, with two ligands $[(RO)_2PO_2]^{2-}$ {R = Et, Bu, 4-$NO_2$-Ph} involved together in holding the dinuclear assembly. As a result of the bridging coordination of the phosphate ligand, the core of the dinuclear nickel complexes contains a puckered eight-membered $Ni_2P_2O_4$ ring. Apart from phosphate ligands, the remaining coordination environment around the two nickel centers in each complex comprises a Tp* ligand. Thus, all complexes present the same coordination environment of both nickel centers (five-coordinate, 3N, 2O coordination environment). The stereochemistry of nickel centers in **1** and **3** is well described as distorted square-pyramidal, and the degree of distortion ($\tau$) can be estimated, according to the Addison method,[25] $\tau = 1$ for an ideal trigonal bipyramid whereas $\tau = 0$ for square-pyramid. The calculated $\tau$ values for **1**

(22) Matsunaga, Y.; Fujisawa, K.; Ibi, N.; Miyashita, Y.; Okamoto, K. *Inorg. Chem.* **2005**, *44*, 325–335.
(23) Santana, M. D.; García, G.; López, G.; Lozano, A.; Vicente, C.; García, L.; Pérez, J. *Polyhedron* **2007**, *26*, 1029–1036.
(24) Moratal, J.-M.; Salgado, J.; Donaire, A.; Jiménez, H. R.; Castells, J. *Inorg. Chem.* **1993**, *32*, 3587.
(25) Addison, A. W.; Rao, T. N.; Reedijk, J.; van Rijn, J.; Verschoor, G. C. *J. Chem. Soc., Dalton Trans.* **1984**, 1349–1356.

**Table 2.** Selected Bond Lengths [Å] and Angles [deg] for Complexes **1**−**3**

| | **1**[a] | **2**[b] | **3**[c] |
|---|---|---|---|
| Ni(1)−N(1) | 2.008(4) | 2.063(2) | 2.006(3) |
| Ni(1)−N(3) | 2.075(4) | 2.024(3) | 2.026(4) |
| Ni(1)−N(5) | 2.042(4) | | 2.027(3) |
| Ni(1)−O(1) | 2.000(3) | 2.0045(18) | 2.000(3) |
| Ni(1)−O(2) #1 | 1.991(3) | | 2.057(3) |
| Ni(1)−N(1) #1 | | 2.063(2) | |
| Ni(1)−O(1) #1 | | 2.0045(18) | |
| N(1)−Ni(1)−N(3) | 92.11(15) | 92.22(9) | 96.54(13) |
| N(1)−Ni(1)−N(5) | 92.07(15) | | 88.71(13) |
| N(1)−Ni(1)−O(1) | 103.32(15) | 90.08(8) | 104.27(13) |
| N(1)−Ni(1)−O(2) #1 | 105.21(15) | | 96.53(11) |
| N(3)−Ni(1)−N(5) | 85.12(17) | | 85.83(13) |
| N(3)−Ni(1)−O(1) | 163.84(14) | 105.42(8) | 159.19(12) |
| N(3)−Ni(1)−O(2) #1 | 90.04(14) | | 89.15(12) |
| N(5)−Ni(1)−O(1) | 89.49(15) | | 94.53(12) |
| N(5)−Ni(1)−O(2) #1 | 162.23(13) | | 173.14(12) |
| O(1)−Ni(1)−O(2) #1 | 90.52(12) | | 88.50(11) |
| N(1)−Ni(1)−N(1) #1 | | 85.07(11) | |
| N(1)−Ni(1)−O(1) #1 | | 161.89(9) | |
| N(3)−Ni(1)−N(1) #1 | | 92.22(9) | |
| N(3)−Ni(1)−O(1) #1 | | 105.42(8) | |
| N(1) #1-Ni(1)−O(1) | | 161.89(9) | |
| N(1) #1-Ni(1)−O(1) #1 | | 90.08(8) | |
| O(1)−Ni(1)−O(1) #1 | | 89.17(10) | |

[a] Symmetry transformations #1 $-x, -y+1, -z$. [b] Symmetry transformations #1 $x, y, -z$. [c] Symmetry transformations #1 $-x+1, -y+2, -z+1$.

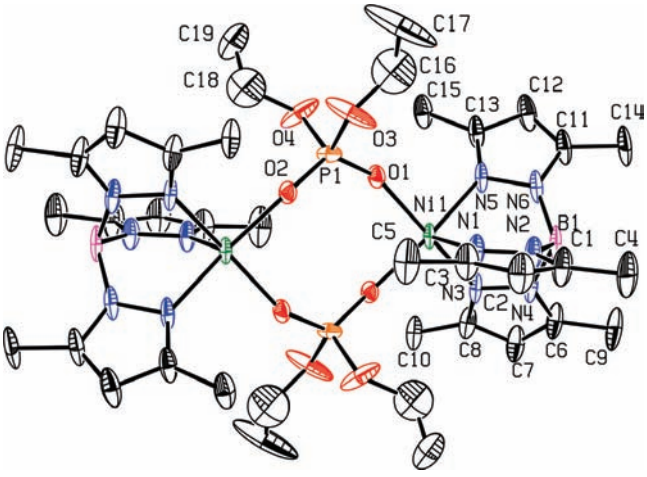


**Figure 3.** ORTEP drawing of complex **1** (ellipsoids at 50% probability level) with atom-labeling scheme.

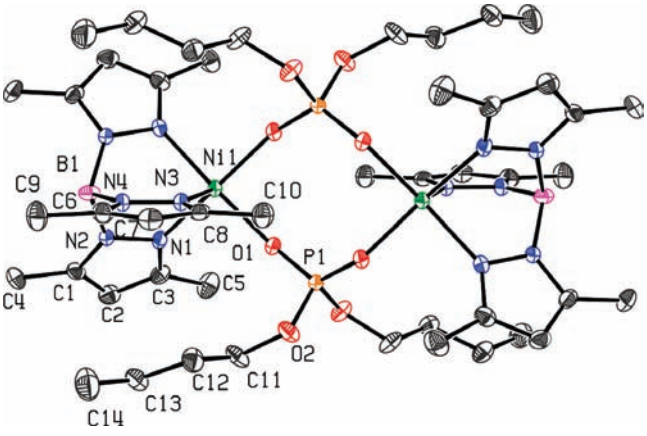


**Figure 4.** ORTEP drawing of complex **2** (ellipsoids at 50% probability level) with atom-labeling scheme.

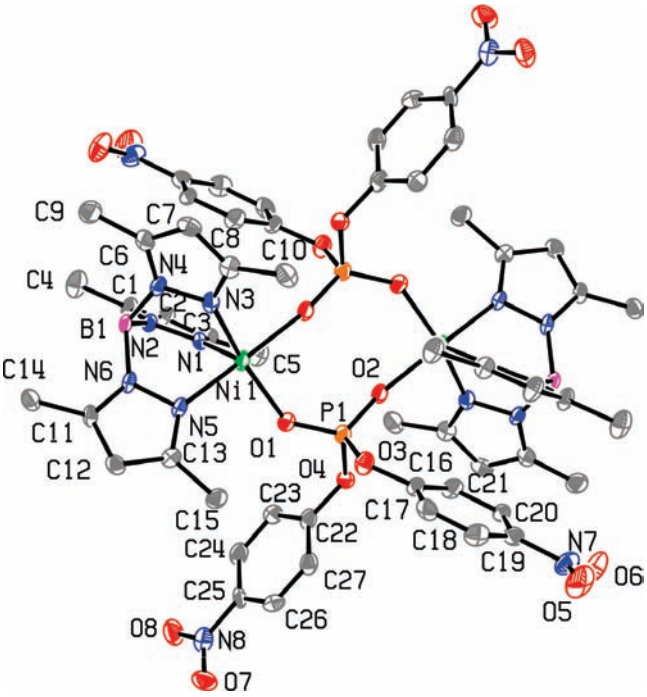


**Figure 5.** ORTEP drawing of complex **3** (ellipsoids at 50% probability level) with atom-labeling scheme.

and **3** are 0.04 and 0.23, respectively, whereas for **2** it is 0, that is, a square-pyramid. In each case, its corresponding basal plane comprises two nitrogen atoms of Tp* ligand and two oxygen atoms of the phosphate ligands, and the axial site is occupied by the third nitrogen atom of Tp*. Nickel atoms in these complexes are displaced out of the basal plane 0.4998, 0.3179, and 0.3584 Å for **1**, **2**, and **3**, respectively. Ni−N distances are not significantly different (2.006−2.076 Å) from those observed in pentacoordinate complexes of nickel(II) containing tris(pyrazolyl)-borate ligands.[12,21,26] Ni−O bond lengths are between 1.991−2.057 Å as others previously found for five-coordinate nickel complexes.[27] The most probable conformation for each eight-membered $Ni_2P_2O_4$ ring was established using specifically the *RingConf* software with $\sigma = 10°$.[28] The conformation is *twist-chair*, distorted 41°, 27°, and 32° for **1**, **2**, and **3**, respectively.

The most relevant supramolecular feature of complex **1** is its polymeric structure supported by hydrogen bonds which link the oxygen atoms from the OEt group and H atoms of the methyl groups at Tp*. Each centrosymmetric complex yields four hydrogen bonds along the chain. Some weaker interactions complete the intermolecular forces (Supporting Information, Figure S1). Complex **2** also adopts a chain structure, in this case complementary hydrogen bonds link oxygen atoms from the OBu group and H atoms of the α-methylene groups at OBu group of the next dimer. Each centrosymmetric ($D_{2h}$) complex yields eight hydrogen bonds along the chain

(26) Ruman, T.; Łukasiewicz, M.; Ciunick, Z.; Wołowiec, S. *Polyhedron* **2001**, *20*, 2551.
(27) Yakovenko, A. V.; Kolotilov, S. V.; Addison, A. W.; Trofimenko, S.; Yap, G. P. A.; Lopushanskaya, V.; Pavlishchuk, V. V. *Inorg. Chem. Commun.* **2005**, *8*, 932–935.
(28) Kessler, M.; Pérez, J.; Bueso, M. C.; García, L.; Pérez, E.; Serrano, J. L.; Carrascosa, R. *Acta Crystallogr., Sect. B* **2007**, *63*, 869–878.

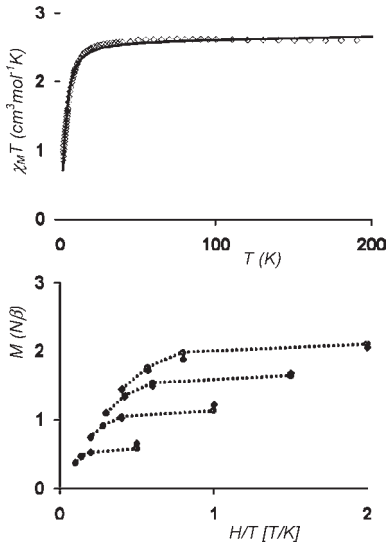


**Figure 6.** Magnetic behavior of complex **2**: (a) Thermal dependence of $\chi_m T$; (b) Reduced magnetization taken from 1 to 4 T and from 2 to 10 K. Fits to the experimental data (diamonds) are shown as open circles for parameters given in the text. Dotted lines are only guides for eyes.

**Table 3.** Magnetic Fitting Results for Complexes **1**−**5**

| | **1** | **2** | **3** | **4** | **5** |
|---|---|---|---|---|---|
| $C_m$ ($cm^3K/mol$) | 2.56 | 2.62 | 2.27 | 2.40 | 2.48 |
| $\theta$ (K) | −0.6 | −0.7 | −0.7 | −0.8 | −0.5 |
| $g$ | 2.26 | 2.25 | 2.13 | 2.19 | 2.23 |
| $J$ ($cm^{-1}$) | −0.5 | −0.5 | −0.4 | −0.4 | −0.4 |
| $D$ ($cm^{-1}$) | 8.5 | 9.0 | 4.4 | 9.0 | 7.9 |
| $R$ | $2 \times 10^{-4}$ | $1.5 \times 10^{-3}$ | $2 \times 10^{-4}$ | $1 \times 10^{-3}$ | $3 \times 10^{-4}$ |
| $D_{max}$ ($cm^{-1}$) | 11.7 | 12.5 | 8.1 | 11.7 | 10.5 |

(Supporting Information, Figure S2). The supramolecular structure of **3** is more complicated. Each phosphate ligand has two $NO_2$-Ph groups at 74.11° (Figure 5) that afford an intricate three-dimensional network by hydrogen bonds using the oxygen atoms of nitro groups.

**Magnetic Properties.** Susceptibility and magnetization measurements reveal a similar behavior for all the studied compounds. The magnetic data for complex **2** are plotted in Figure 6, whereas the curves for the rest of the compounds are included as Supporting Information. In all cases, Curie−Weiss behavior is observed in the temperature range 300−30 K, leading to $C_m$ values from 2.27 to 2.62 (see Table 3), fact that is consistent with S = 1 ground states, as expected for Ni(II) pentacoordinate compounds. Below 30 K, the deviation from the Curie−Weiss law, as well as the decrease of the magnetic effective moment, indicate that antiferromagnetic interactions and/or zero-field splitting of the single ion triplet state are operatives. At the same time, the magnetization per formula unit taken at low temperature ($T$ = 2 K) saturates well below the purely paramagnetic value $M_{mol}/N\mu_B = 4$, which again suggests the presence of a sizable zero-field splitting.

The susceptibility and magnetization data were analyzed on the basis of the following spin Hamiltonian:

$$H = -2JS_1 \cdot S_2 + D({S_{1z}}^2 + {S_{2z}}^2) - g\mu_B B(S_1 + S_2)$$

where the first term accounts for the isotropic exchange interaction, the second one express the axial single-ion zero-field splitting of nickel(II) ions, and the third one is the Zeeman effect considering an isotropic $g$ value. The introduction of a mean field correction term to take into account interdimer contacts via hydrogen bonds was also considered, but this term was finally disregarded considering the low value obtained for the intradimeric exchange parameters in all cases.

Two sets of magnetic data, $\chi(T)$ and $M(B)$, were fitted using exact diagonalization of the energy matrix for $S_1 = S_2 = 1$. The best-fit parameters obtained by minimizing the reliability $R$ factor $R = \sum[(\chi_m T)^{exp} - (\chi_m T)^{cal}]^2 / \sum[(\chi_m T)^{exp}]^2$ are listed in Table 3. As shown Figure 6, calculated curves reproduce very well magnetic data in the whole investigated temperature range.

The obtained $g$ values from data fitting are in good agreement with those from Curie constants. As usual, they exhibit a positive moderate deviation with respect to the free-electron value because of spin−orbit coupling. Calculated $J$ parameters are extremely low and negatives, as expected because of the large exchange pathways via phosphate groups. But, as shown the results above, it appears that magnetic behavior of these pentacoordinate Ni(II) dimers is dominated by magnetic anisotropy of single ions instead of exchange interactions. Calculated $D$ values are relatively large and its effect on magnetic susceptibility curves is more pronounced than those that are due to isotropic intradimeric exchange. In fact, good agreements between calculated and experimental curves could be obtained for all compounds considering only non-interacting $S = 1$ ions in the presence of a single ion anisotropy. Experimental data fitted by the following equation allow us to determine the maximum values for the $D$ factors ($D_{max}$ in Table 3) where $x = D/kT$.[29]

$$\chi_m = \frac{2Ng^2\beta^2}{3kT}\left[\frac{2/x - 2\exp(-x)/x + \exp(-x)}{1 + 2\exp(-x)}\right]$$

It is worth mentioning that they show roughly the same tendency than those calculated using the whole Hamiltonian. But, in any case, the magnetic interactions cannot be absolutely neglected taking into account that variable temperature solid-state $^{31}P$ NMR studies have provided direct evidence of the involvement of phosphate bridging anions in the spin transfer between transition metal ions.[30]

Even if the magnetic data taken and their analysis have been done uniformly for all the samples, we must recognize that powder susceptibility curves do not have enough resolution to provide a unique and unambiguous solution. Other sets of parameters with slightly lower values of $J$ and higher values of $D$ (with the $D_{max}$ limits) can also give rise to acceptable agreements between experimental and calculated data. Moreover, the presence in these compounds of interdimer contacts via hydrogen bonds can introduce an additional degree of uncertainty about the calculated $D$ values. It is well established that the effect of a positive value of single-ion zero-field splitting on the magnetic effective moment at low temperatures is qualitatively similar to that derived from negative molecular

(29) Landee, C. P.; Mudgett, D. M.; Foxman, B. M. *Inorg. Chim. Acta* **1991**, *186*, 45–49.

(30) (a) Lezama, L.; Suh, K. S.; Villeneuve, G.; Rojo, T. *Solid State Commun.* **1990**, *76*, 449. (b) Roca, M.; Amorós, P.; Cano, J.; Marcos, M. D.; Alamo, J.; Beltrán-Porter, A.; Beltrán-Porter, D. *Inorg. Chem.* **1998**, *37*, 3167–3174.

**Table 4.** Comparison between Structural and Magnetic Data of Five-Coordinated Dimeric Phosphate-Bridged Ni(II) Complexes

| compound | $d_{Ni-Ni}$ (Å) | $d_{Ni\text{-}b\text{-}Ni}$ (Å) | $a^a$ | $d_{Ni\text{-}Nax}$ (Å) | $d_{Ni\text{-}Oeq}$ (Å) | $\tau$ | $h_{Ni}$ (Å) | rms | $d_{out}$ (Å)$^b$ | $d_{in}$ (Å)$^b$ | $J$ (cm$^{-1}$) | $D$ (cm$^{-1}$) |
|---|---|---|---|---|---|---|---|---|---|---|---|---|
| [NiTp*($\mu$-$O_2P(OEt)_2$)]$_2$ (**1**) | 5.246 | 6.937 | 0.756 | 2.008 | 2.000<br>1.991 | 0.04 | 0.50 | 0.17 | 0.18 | 0.12 | −0.5 | 8.5 |
| [NiTp*($\mu$-$O_2P(OBu)_2$)]$_2$ (**2**) | 5.171 | 6.992 | 0.739 | 2.024 | 2.005 | 0 | 0.32 | 0.24 | 0.28 | 0 | −0.5 | 9.0 |
| [NiTp*($\mu$-$O_2P(OPh\text{-}4\text{-}NO_2)_2$)]$_2$ (**3**) | 5.383 | 7.002 | 0.768 | 2.006 | 2.000<br>2.057 | 0.23 | 0.36 | 0.09 | 0.03 | 0.32 | −0.4 | 4.4 |
| [NiTp*($\mu$-$O_2P(OMe)_2$)]$_2$ (**4**) | 5.232 | 6.968 | 0.750 | 2.008 | 2.023<br>1.967 | 0.31 | 0.31 | 0.17 | 0.18 | 0.14 | −0.4 | 9.0 |
| [NiTp*($\mu$-$O_2P(OPh)_2$)]$_2$ (**5**) | 5.357 | 6.994 | 0.766 | 2.021 | 2.056<br>1.972 | 0.24 | 0.27 | 0.13 | 0.11 | 0.13 | −0.4 | 7.9 |

[a] $a = d_{Ni-Ni}/d_{Ni\text{-}b\text{-}Ni}$. $h_{Ni}$ is the nickel height from the basal plane. [b] $d_{in}$ and $d_{out}$ are the relative in-plane and out-of-plane displacement of the Ni(II) ion, respectively.

field correction used to account for the isotropic exchange interaction with nearest neighbors.[31] However, it is noteworthy that for compounds **1**−**5** the observed decreases on the magnetic effective moment at low temperatures can only be fitted with unrealistic values for the interdimer interactions ($z'J' > 10$ cm$^{-1}$) if the $D$ term is not included. On the other hand, all the compounds are silent from 4 to 300 K in conventional $X$-band (9.5 GHz) and $Q$-Band (34 GHz) EPR measurements. Thus, we can confirm not only the presence of the zero-field splitting but also that magnitudes are higher than incident microwave energy. High-field high-frequency EPR measurements should be desirable to unambiguously determine the sign and magnitudes of $D$, but simultaneous fits of variable temperature susceptibility and variable field magnetization can also provide accurate $D$ values.[32] In this sense, we have confidence in both the sign and the magnitude of the calculated values of $J$ and $D$.

The main structural and magnetic data of the five-coordinate dimeric phosphate-bridged Ni(II) complexes are collected in Table 4. Even if the number of known compounds is too limited to establish true magneto-structural correlations at this stage, we have tried to extract some conclusions from a comparative analysis. With respect to the exchange parameters, the low and negative values calculated are characteristics of $\mu$-(O,O′)$PO_4$ bridges. According to Goodenough's[33] rules, antiferromagnetic exchange should be expected for interactions propagated via this type of bridges. In addition, the displacement of the metal ions from the exchange plane is usually one of the most important factors affecting the magnitude of the $J$ parameter. For vanadyl phosphates with $\mu$-(O,O′)$PO_4$ bridges, Roca et al.[30b] have predicted that the magnetic exchange should be more sensitive to in-plane relative displacements than to out-of-plane movements. A different behavior was expected for the present compounds taking into account that the magnetic orbital is mainly $d_{xy}$ in vanadyl phosphates, while in pentacoordinate Ni(II) complexes with distorted square-pyramidal geometry it is $d_{x^2-y^2}$. In any case, both deviations contribute simultaneously to reduce magnetic orbital overlap giving rise to low $J$ values. In complexes **1**−**5**, Ni(II) in-plane and out-of-plane displacements are inversely correlated, which could explain that all compounds show intradimeric magnetic interactions with almost the same strength.

Magnetic anisotropy of the compounds can also be related to structural features. From data collected in Table 4, it is obvious that calculated $D$ parameters cannot be uniquely correlated neither with weakening of axial bonds, as it is usually considered for octahedral Ni(II) compounds[6], nor with $\sigma$-donor effect of the apical ligand, as observed by Desrochers et al.[34] in four-coordinate nickel(II) scorpionate complexes. Moreover, as magnetic anisotropy should be higher for trigonal-bipyramidal species than for the square-pyramidal, a direct relation between the Addison parameter, $\tau$, and calculated $D$ values was expected, but in these cases it cannot be established. Only a smooth correlation has been found between calculated $D$ values and planarity of the eight-membered $Ni_2P_2O_4$ ring. This behavior can be explained if it is considered that a planar disposition of phosphate bridges favors in-plane covalency and, therefore, it reduces both the orbital contribution to ground state and the axial zero-field splitting term. Thus, it appears that the orbital reduction factor can determine magnetic anisotropy in these particular cases; however, other factors like geometrical distortion or crystal field cannot be neglected. Further studies on analogous compounds with large structure variations should be necessary to confirm this hypothesis.

**Acknowledgment.** Technical and human support provided by SGIker (UPV/EHU, MICINN, GV/EJ, ESF) is gratefully acknowledged. This work is the result of financial support of Fundación Séneca de la Región de Murcia (project 08670/PI/08) and INFO and FEDER up to 80% of the PCTRM 2007-2010. We thank also the Ministerio de Educación y Ciencia for partial financial support (project CTQ2008-02767/BQU). L.L.-B. thanks the Fundación Séneca de la Región de Murcia for a FPI grant.

**Supporting Information Available:** Crystallographic data in CIF format; further details are given in Figures S1−S10. This material is available free of charge via the Internet at http://pubs.acs.org.

(31) (a) Duggan, D. M.; Hendrickson, D. N. *Inorg. Chem.* **1974**, *13*, 2929–2940. (b) Nanda, K. K.; Addison, A. W.; Paterson, N.; Sinn, E.; Thompson, L. K.; Sakaguchi, U. *Inorg. Chem.* **1998**, *37*, 1028–1036.

(32) (a) Herchel, R.; Boca, R.; Krzystek, J.; Ozarowski, A.; Duran, M.; van Slageren, J. *J. Am. Chem. Soc.* **2007**, *129*, 10306–10307. (b) Feng, P. L.; Koo, C.; Henderson, J. J.; Manning, P.; Nakano, M.; del Barco, E.; Hill, S.; Hendrickson, D. N. *Inorg. Chem.* **2009**, *48*, 3480–3492. (c) Costes, J. P.; Yamaguchi, T.; Kojima, M.; Vendier, L. *Inorg. Chem.* **2009**, *48*, 5555–5561.

(33) Goodenough, J. B. *Magnetism and the Chemical Bond*; Interscience: New York, 1963.

(34) Desrochers, P. J.; Telser, J.; Zvyagin, S. A.; Ozarowski, A.; Krzystek, J.; Vicic, D. A. *Inorg. Chem.* **2006**, *45*, 8930–8941.